Replacing Coal and Natural Gas Energy Generation with Carbon-Free Energy Sources in Texas

Jacob Bryan, Aiden Meek

December 15, 2021

Contents

Executive Summary

This report discusses the use of a hybrid energy system (HES) in Texas. The HES replaces all coal and natural gas electricity production in Texas with solar, wind, and nuclear power. The HES also uses thermal and hydrogen storage to minimize overproduction and allow for load following. The system model was required to meet the real load data for Texas in 2020. Wind speed data and solar irradiation data for 2020 were also used by the system model to generate power outputs by solar panels and wind turbines.

Each of the model components were modeled in Dymola using simple thermodynamic equations. An optimization algorithm found an optimum design point, aiming to minimize the system's levelized cost of electricity (LCOE) and meet the demand at all times of the year.

The engineers determined the result from the optimization to be reasonable. The optimized LCOE of the system was \$73.04/MWh if excess hydrogen produced for storage was sold off at a breakeven price. The optimized system requires 61 Natrium reactors, 5317 3.2 MW wind turbines, and 307.9 km^2 of solar panels. The proportions of the total energy produced by each subsystem of the HES is shown in the figure below. A majority of the power came from nuclear power, with the rest being a near even split between wind and solar. The seasonal hydrogen storage contributed only a small portion of the total energy. While this optimized LCOE is much greater than the current LCOE of Texas' power generation, it stops production of greenhouse gases in Texas, and provides green hydrogen to release to the green energy market.

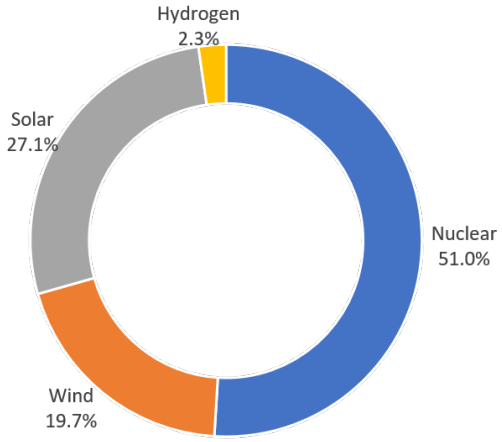

Proportions of energy produced by each generation method for the optimal design point.

1 Introduction

Continuing to rely on fossil fuels for our energy needs results in further carbon emissions and increased CO2 levels in the atmosphere. Society faces the problem of reducing fossil fuel consumption, while maintaining the power generation required to maintain our way of life. Texas has installed significant numbers of wind turbines to help reduce its dependence on fossil fuels. However, Texas still has a significant dependence on fossil fuels that needs to be reduced. The goal of this project is to determine an economically optimized hybrid energy system (HES) that can provide Texas' energy needs while eliminating the need for fossil fuels.

This project aims to eliminate the need for fossil fuel dependence in Texas for electricity production by designing a HES. By increasing solar production, installing more wind turbines, building nuclear reactors, and incorporating energy storage, Texas could become carbon free in its electricity production. The HES design would be capable of meeting Texas' energy demands while minimizing the cost of electricity in the new system.

The HES would be built in, and provide power for, Texas (specifically for the ERCOT power company that provides electricity for nearly all of Texas). Solar would be installed in the west of Texas; additional wind production would likely be installed in the north of Texas. The nuclear reactors could be located anywhere in the state. Thermal energy storage, which allows nuclear reactors to load follow, would be installed on site next to the nuclear reactors. Additional energy storage, in the form of hydrogen, could be installed salt caverns in the north or east of Texas.

To summarize, this project has the following objectives:

- Replace all of the fossil fuel energy sources in Texas with a combination of wind, solar, nuclear, and hydrogen power.
- Determine the optimal sizing of each of these subsystems to minimize the LCOE of the system.
- Ensure that there is never a period of unmet demand during the simulated time frame.

2 Energy Demand and Resources

Texas is a state of both significant energy production, with abundant wind and solar natural resources, and energy consumption, consuming more energy than other other state [1]. Despite these natural resources and having two large nuclear energy facilities, Texas still derives 63.7% of its energy from fossil fuel sources via a combination of coal and natural gas, as of 2020 [2].

With the goal to replace these coal and natural gas generation facilities with carbon-free alternatives – namely a combination of wind, solar, nuclear, and hydrogen fuel cells – the demand profile which the new HES must meet is determined by subtracting the energy generated from green energy sources from the total demand. This section will examine this demand profile and consider the wind and solar potential of the state through a look at the wind speed and solar irradiance at multiple locations in the state.

2.1 Demand Profile

The demand profile which the HES at hand is required to meet is equal to the total demand from the ERCOT data, minus the energy generated from existing carbon-free energy sources. A plot of this residual demand signal can be seen in Fig. 1.

The residual demand profile has a number of interesting characteristics. First, the demand increases significantly over the summer months, peaking in August. The demand is often 50-100% higher during the summer compared to the rest of the year. This seasonal variation poses a significant difficulty when trying to design a HES with a significant portion of must-run nuclear power, as sizing the system to meet summer demand peaks will invariably result in significant energy overproduction during the winter, spring, and fall. Alternatively, extreme levels of seasonal energy storage may be required to meet the demand during summer if the HES is sized more appropriately (i.e. smaller) for the remainder of the year.

The difference in demand profile during each season is further illustrated in Fig. 2, which shows hourly average demand profiles for January, April, July, and October. Energy consumption in July is significantly

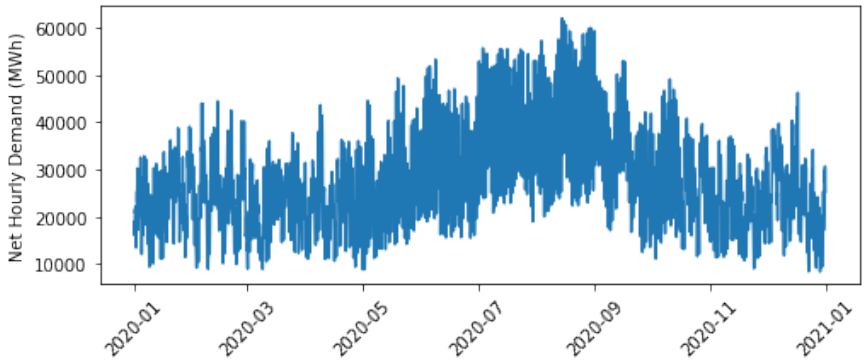

Figure 1: Residual demand profile for ERCOT in 2020.

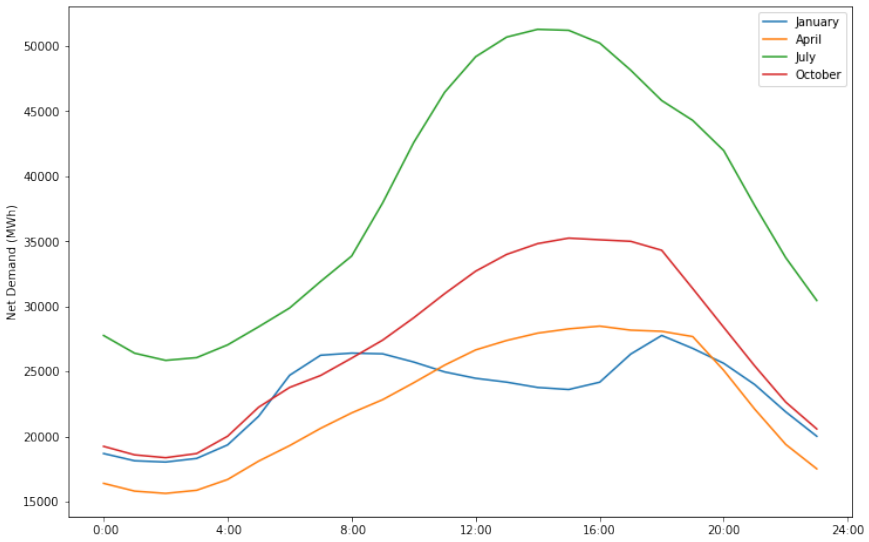

Figure 2: Average hourly demand profiles for January, April, July, and October.

higher than in the other three example months. Also of note is how the January profile is bimodal, with peaks around 7:00 am and 6:00 pm, while the other months are unimodal.

2.2 Wind and Solar Resources

Wind speed and solar irradiance data were collected from NASA POWER, using the 50-m height (parameter "WS50M") for wind speed and all-sky surface shortwave downward irradiance (parameter "ALLSKY_SFC_SW_DWN") for global horizontal irradiance (GHI) [3]. In an effort to make the data collected for wind speed and GHI less dependent on a specific location and more representative of a region, data from several locations were sampled from the regions of interest for each resource and averaged. The locations of the sampled points are shown on the map in Fig. 3. Note that due to the 0.5°-by-0.5° (approximately 40 miles by 40 miles) resolution of the NASA POWER data, much finer sampling of the region is not particularly useful. Also, this somewhat coarse resolution also means that the data from each location already represents a spatial average of the surrounding area. Hourly averaged profiles for wind speed and GHI are shown in Fig. 4.

Wind speed at 50 meters has fairly significant seasonal variation. Two crucial observations can be made from 4a. First, wind speed tends to be higher at night than during the day. This is advantageous, as wind production will typically increase at night, when solar panels are no longer producing electricity. However, the average wind speed in the plot is lowest for July, when demand is at its highest, potentially increasing

Figure 3: Locations sampled for wind (blue markers) and solar (red markers) data.

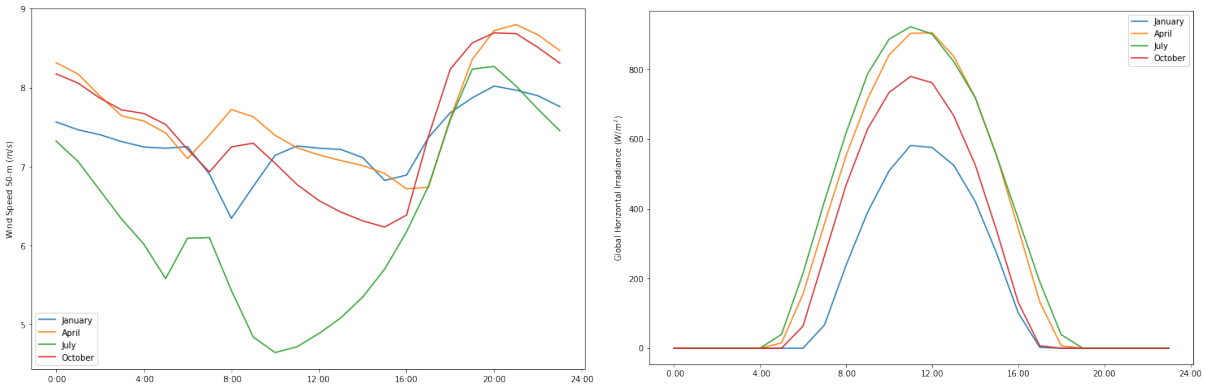

(a) Wind Speed

(b) GHI

Figure 4: Hourly averaged wind and solar data for January, April, July, and October.

the effective seasonal variation in demand that must be met by other resources. The annual average wind speed in Texas is still one of the most favorable for wind energy in the nation; the sampled data have an average of 7.25 m/s.

GHI varies both daily, as the sun rises and sets, and seasonally over the course of the year with the changing elevation angle of the sun. In Fig. 4b, it can be seen that GHI drops to zero during the night, as expected, with daytime peaks being lowest in the winter and highest in spring and summer. The maximum value in the curve for July is 923 $\mathrm{W/m^2}$. While there is some variability in day-to-day GHI due to cloud cover, GHI is typically more predictable than wind speed since the daily and seasonal movement of the sun is very well understood.

2.3 Salt Deposits for Hydrogen Storage

Texas has large salt deposits in the north and the east of the state. These salt deposits shown in Fig. 5 could be used as geologic hydrogen storage. Hydrogen is typically stored in artificial salt caverns, but salt mines or natural cavities in the salt could also be used. In this project, the engineers assumed 20 artificial caverns as the cap on hydrogen storage.

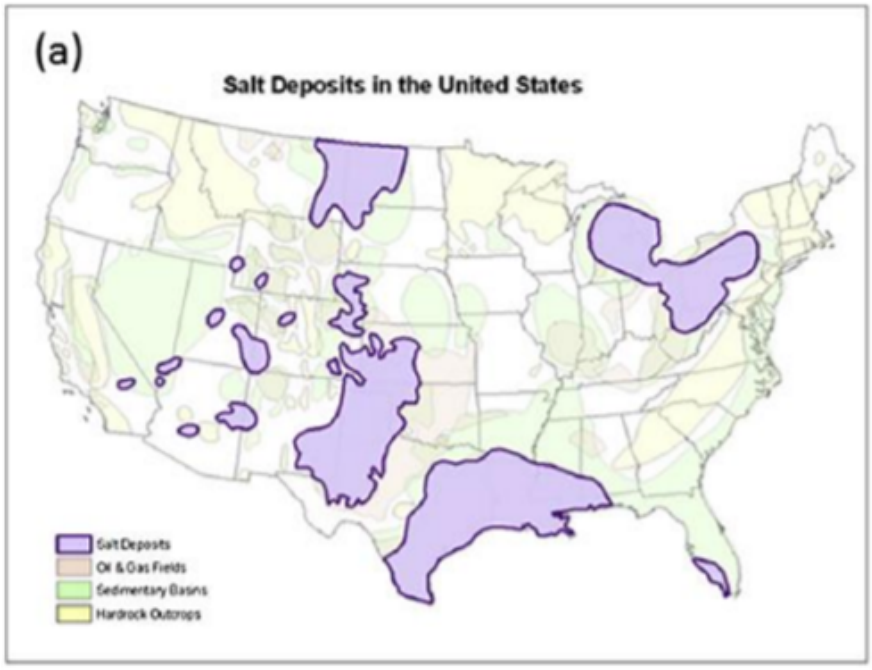

Figure 5: Salt deposits in the United States [8].

Each artificial cavern, as described by Ahluwalia, et al. [8] holds up to 6000 metric tons of hydrogen. The caverns contain high pressure (50 - 150 bar) hydrogen. Artificial salt caverns are made by drilling holes, and pumping water. The water dissolves the salt deposit gradually creating an artificial cavity in the salt. The holes allow for fresh water to be pumped in, and brine to be pumped out. This process is illustrated in Fig. 6.

3 System Designs and Modeling

Given the significant wind and solar resources present in Texas, the proposed HES design includes both wind turbines and photovoltaic solar panels. However, these resources are intermittent and non-dispatchable; the HES uses nuclear power to complement these renewables. Specifically, the Natrium system developed by GE Hitachi Nuclear and TerraPower is used here due its ability to vary power output through its integrated molten salt thermal storage system. This thermal storage is useful short-term energy storage. Hydrogen storage is used for long-term storage in this design, with storage in natural underground reservoirs. The proposed HES is modeled using Dymola, a software for modeling dynamic systems using the Modelica language. Models for each subsystem - Natrium, wind, photovoltaic solar, hydrogen storage, and hydrogen fuel cells - were developed and integrated in this software.

The model the engineers developed uses nuclear, solar, and wind power along with thermal and hydrogen energy storage to meet Texas' energy demands. Natrium Fast Reactors provide the nuclear power and incorporate thermal energy storage. Photovoltaic solar panels and wind turbines use the natural resources in Texas. Hydrogen energy storage takes the excess power to make hydrogen to be stored or sold, and when there is a net demand on the grid, the hydrogen generates power. This system is shown in Fig. 7.

3.1 Natrium

The Natrium system operates a 840-MWt sodium fast reactor as its primary heat source. The reactor is cooled by molten nitrate salt, which is stored in a two-tank storage system. The molten salt can be drawn from the hot storage tank through a salt-steam heat exchanger to drive a steam cycle, outputting 345 MWe at steady state operation. The salt storage capacity allows for more fluid to be drawn from the hot storage tank

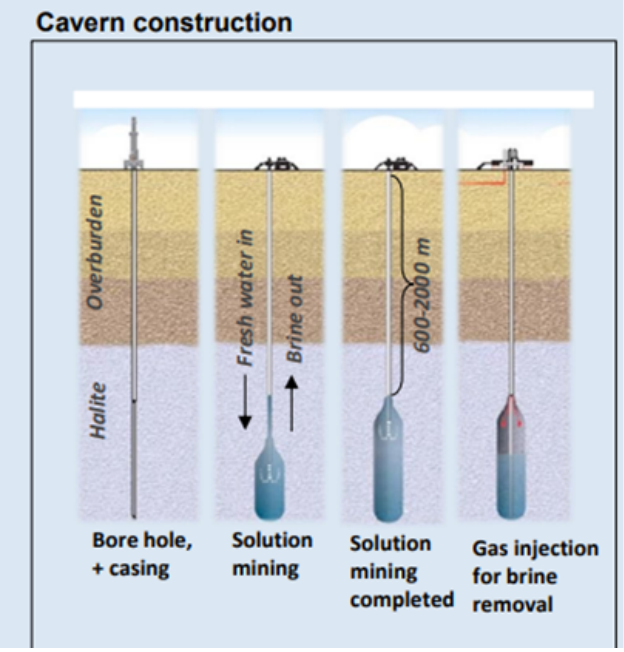

Figure 6: Construction of artificial salt caverns [8].

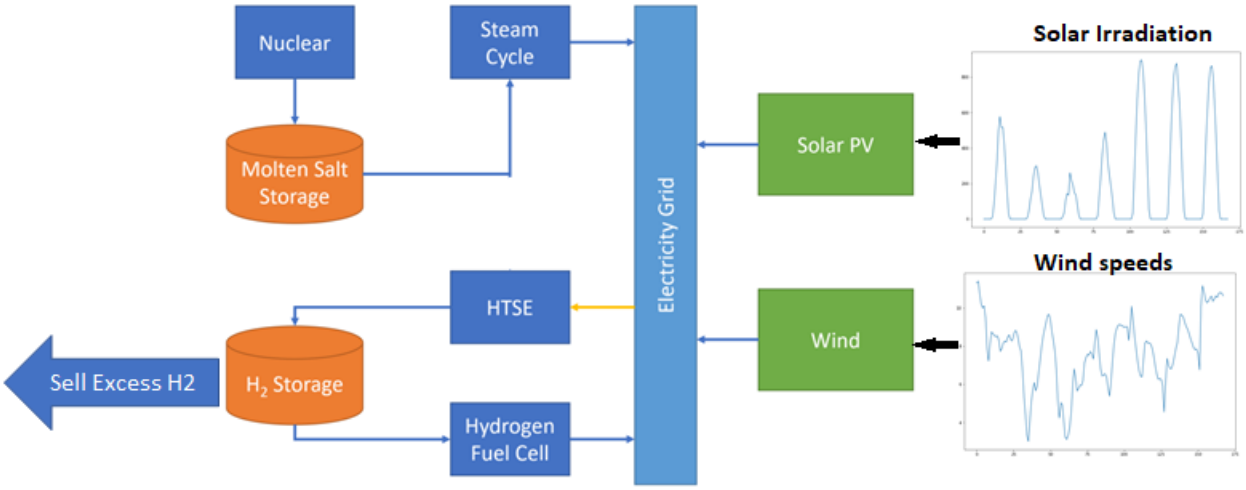

Figure 7: System overview of the model

than in being replaced for a limited duration, resulting in a temporarily increased power output. Natrium is designed to boost the power output to 500 MWe for up to 5.5 hours. The maximum power output is limited by the steam turbine used in the steam cycle, while the duration of the power boost is governed by the hot salt storage capacity.

While Natrium is intended to use molten nitrate salt (60% NaNO3, 40% KNO3) as its primary coolant and thermal storage medium, the model uses constant property liquid sodium for simplicity. While not a perfect substitute, the Natrium model is implemented as a zero-dimensional model, and the thermophysical properties of the fluid will only manifest themselves in the mass flow rates and volume of fluid required for thermal storage. The energy production, storage, and dispatch behavior is independent of the working fluid in the model.

In the model, the storage tank temperatures remain fixed at 490 °C and 300 °C in the hot and cold storage

tanks, respectively. The mass flow rate through the reactor ($\dot{m}_r$) is assumed to be constant and equal to

$$\dot{m}_r = \frac{\dot{Q}_{in}}{c_p(T_H - T_C)},$$

where $\dot{Q}_{in} = 840MW$, c_p is the specific heat capacity of the coolant, and T_H and T_C are the hot and cold storage tank temperatures. It is assumed that the heat of the fluid can be converted to electricity at 41% efficiency (η) through use of a steam cycle. The output power then depends on the mass flow rate through the primary heat exchanger of the steam cycle, $\dot{m}_{hx}$. This mass flow rate is allowed to vary sufficiently such that $0 \leq \dot{W}_{out} \leq 500\,\text{MW}$ and is controlled so that the output power matches the demand as closely as possible. Note that in cases where all of the molten salt is in one tank or the other, it may be necessary to maintain $\dot{m}_{hx} = \dot{m}_r$ in order to ensure that cool fluid is available to cool the reactor.

Summarizing this model into a system of equations,

$$\begin{aligned}
\frac{dm_H}{dt} &= \dot{m}_{hx} - \dot{m}_r \\
\frac{dm_C}{dt} &= \dot{m}_r - \dot{m}_{hx} \\
\dot{m}_{hx} &= \begin{cases} \dot{m}_r & \{m_C = 0 \text{ and } D(t) \leq 345\,\text{MWe}\} \text{ or } \{m_H = 0 \text{ and } D(t) \geq 345\,\text{MWe}\} \\ 0 & m_C > 0 \text{ and } D(t) < 0 \\ \frac{500}{345}\dot{m}_r & m_H > 0 \text{ and } D(t) > 500\,\text{MWe} \\ \frac{D(t)}{\eta c_p(T_H - T_C)} & \text{otherwise,} \end{cases} \\
\dot{W}_{out} &= \eta \dot{m}_{hx} c_p (T_H - T_C),
\end{aligned}$$

where $D(t)$ is the net demand to be met by the nuclear reactor at time t. The initial mass of fluid in each tank is assumed to be equal, so $m_C(0) = m_H(0) = m_{tot}/2$, though this is arbitrary. Both the hot and cold tanks are able to hold the full mass of fluid in the system.

3.2 Wind Turbine

Northern Texas has a great capacity for wind turbines to be installed. The engineers modeled the wind turbines using Dymola. The 2020 wind data collected for north Texas fed into the model, which then generated the power output of the wind installation.

The engineers used a simple model of the wind turbines in the system model. The power output generated follows Eq. 1, which is dependent the power curve function and number of turbines. The equation for power output follows the power curve function for the GE 3.2 MW wind turbines which is dependent on wind speed Fig. 8 shows the power curve function $P_{WT}(v)$.

$$P_{wind} = N_{turbines} \cdot P_{WT}(v) \tag{1}$$

3.3 Solar Panel

Western Texas is a significant solar resource for the state. The engineers modeled the solar panels using Dymola. To reduce complexity the Dymola model uses horizontal solar panels. This assumption simplified the use of the NASA POWER hourly solar data available, since the values are reported as global horizontal irradiance (GHI). The model used solar panels with 15% efficiency. The model uses a simple combination of solar data, panel efficiency, and panel area that follows Eq. 2.

$$P_{out} = \eta G_{in} A_{panel} \tag{2}$$

The incoming solar irradiance is updated every hour for the model, since the data is in hourly steps. The power going out then gets put into "the grid" in the model.

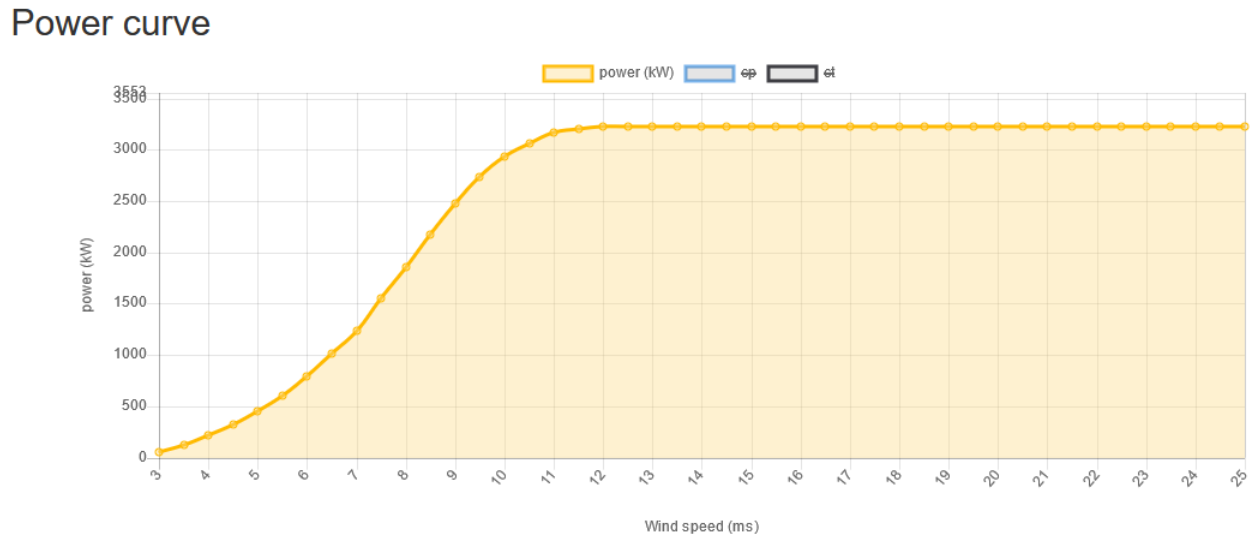

Figure 8: Power curve for a GE 3.2-MW wind turbine [4].

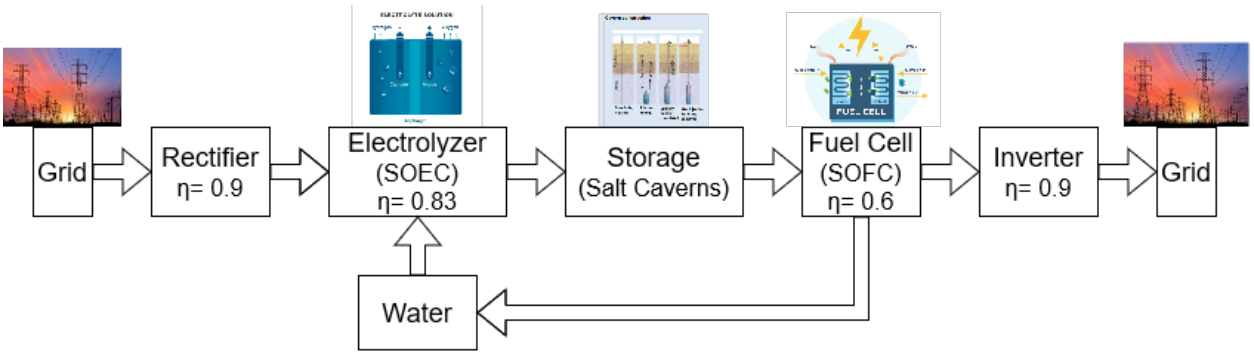

Figure 9: Diagram depicting hydrogen storage process.

3.4 Hydrogen Storage

Texas has large salt deposits that can be used to store excess energy present in the grid for later use. Using hydrogen storage requires 3 steps: electrolysis (breaking water into O2 and H2 in an electrolyzer), storage, and electricity generation (recombination of O2 and H2 in a fuel cell). In addition to these steps, the electricity must be converted at the front and back end of this process. Electrolysis uses and fuel cells generate DC electricity, so to be compatible with the grid, an inverter and a rectifier must be used.

The first step in hydrogen storage requires performing electrolysis. The model for the electrolyzer uses an efficiency of 0.83, which can be obtained by a Solid Oxide Electrolysis Cell (SOEC) [5]. This efficiency is applied to the electricity that comes through the inverter. This means that 83% of the electricity applies towards the higher heating value (HHV) of hydrogen, to produce a certain mass of hydrogen. The efficiencies are applied in Eq. 3. This hydrogen is then passed to storage.

$$\dot{m}_{in,H_2} = \frac{\eta_{rectifier}\eta_{SOEC}P_{grid,excess}}{HHV_{hydrogen}} \tag{3}$$

The second step of hydrogen storage is the storage. Every hour when the grid has excess power, hydrogen is produced. When the grid has a net demand, hydrogen is removed from the storage to meet that demand. Phrased as a differential equation, Eq. 4 shows how this is done. When the hydrogen storage reaches capacity, excess hydrogen is sent off to be sold rather than stored.

$$\frac{dm_{stored}}{dt} = \dot{m}_{in,H2} - \dot{m}_{out,H2} - \frac{dm_{sold}}{dt} \tag{4}$$

The final step in using hydrogen storage for grid power is the fuel cell. This model uses a Solid Oxide Fuel Cell (SOFC) The hydrogen generates electricity in the fuel cell as the hydrogen is converted to water. When the grid has a net demand, the model pulls hydrogen out at a rate sufficiently high to meet that demand. The fuel cell process has an efficiency of 0.60 and Eq. 5 models this conversion. The model uses this efficiency as well as the HHV of hydrogen to determine the amount of electricity. The electricity produced is then passed to the inverter to send the electricity to the grid in a form that the grid can accept.

$$P_{grid,demand} = P_{fuelcell} = \eta_{inverter}\eta_{fuelcell}\dot{m}_{out,H2}HHV_{hydrogen} \tag{5}$$

The model capped the maximum power released by the fuel cell due to concerns that excessive installed fuel cell capacity would be unrealistic. The power output of the fuel cell was capped at 35.5 GW, with 2556 GWh of storage. This allows the storage to be emptied in 3 days if run at full capacity.

This hydrogen model assumes that using the HHV of the hydrogen is okay. In reality, the LHV would be more appropriate since both the SOEC and the SOFC operate around 750 °C. However, since the model uses the value on both the front end and back end of the cycle, the difference may not be very significant. In fact, because far more hydrogen is produced by the SOEC than the SOFC, using the HHV provides a conservative estimate of how the system will perform.

The system also assumes the SOEC's and SOFC's have a ramp up and ramp down time much less than an hour. In the model this translates to having instant response time to changes in supply and demand. SOEC's and SOFC's must be held at constant temperature at all times, so response time is not affected by needs to heat the system. The heat required to maintain the SOEC and SOFC at temperature are not accounted for in this model.

3.5 Secondary Hydrogen Applications

The excess hydrogen produced by this setup needs to be sold or used. Green hydrogen can be sold for prices between $2.50-6.80; the model uses these values to calculate the LCOE of the system. The hydrogen produced needs to be sold at $6.38 for a breakeven price, if sold for more than that, the LCOE is reduced. If sold for less, the LCOE increases in order to offset the cost of selling hydrogen at a loss.

The global hydrogen market is 98.8 billion kg H2. This is broken into several categories, some of which are shown in Fig. 10. The world's chemical market consumes most of the hydrogen produced in the production of petroleum, ammonia, and methanol. Transportation is likely to demand more hydrogen in coming years. The hydrogen produced could go to several of these sources.

A more broken-down view of the different categories can be seen in Fig. 11, from the Atlas of Energy Transition. The categories used here are fuel, chemical and industry. Various uses are shown under each category.

This system produces 1.8 billion kg of excess hydrogen (2% of the world demand) every year. While this may be a massive amount, a hydrogen market report predicts the world demand for hydrogen to more than double in the next 10 years. This green hydrogen would contribute significantly to that growing need.

4 Simulations and Design Optimization

The optimal HES design is defined as the one which minimizes the levelized cost of energy (LCOE) of the system. To calculate this system-level LCOE (denoted LCOE_{sys}), a weighted sum of the subsystem LCOEs is taken according to the amount of energy produced by each subsystem, giving a levelized annual cost of energy generation. Then, the revenue from sold hydrogen is subtracted from the annual cost, and the difference is normalized by the total annual energy demand. In other words,

$$\text{LCOE}_{sys} = \frac{\sum_{i=1}^{N} \text{LCOE}_i E_i - P_{H2} m_{H2}}{D_{tot}}, \tag{6}$$

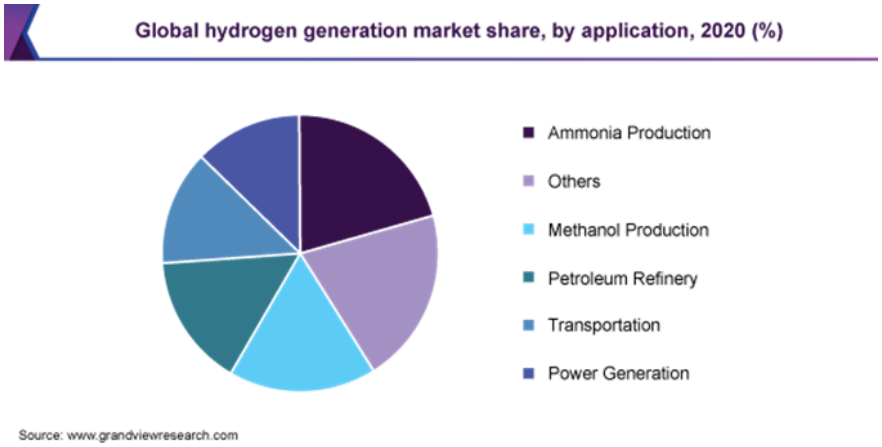

Figure 10: Global hydrogen use by category [6].

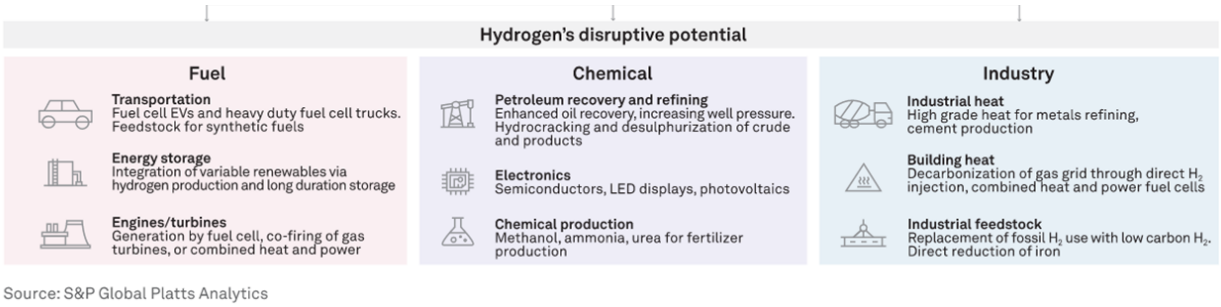

Figure 11: Various uses of hydrogen under the three main categories [7].

where $D_{tot} = \int_{t_0}^{t_f} D(t)dt$, $E_i = \int_{t_0}^{t_f} E_i(t)dt$, m_{H2} is the mass of hydrogen sold, P_{H2} is the average price of that sold hydrogen, and the summation term in the numerator includes terms for the nuclear, wind, solar, electrolysis, hydrogen storage, and hydrogen fuel cell subsystems. The LCOEs used for each subsystem is given in Table 1. Note, however, that the LCOE of each subsystem depends on its capacity factor. The capacity factor assumed for each subsystem is included in the table.

The sizing of the HES is parameterized by three design variables: the number of nuclear reactors ($N_{nuclear}$), the number of wind turbines (N_{wind}), and the solar panel area (A_{solar}). Let these form a point in the design space

$$\vec{x} = [N_{nuclear},\ N_{wind},\ A_{solar}]\,.$$

Subsystem	LCOE ($/MWh)	Capacity Factor (%)
Nuclear	70.59	90
Wind	36.93	41
Solar PV	30.43	29
Electrolysis	50.00	25
H2 Storage	20.00	–
Fuel Cell	50.00	25

Table 1: HES subsystem LCOE values [5, 8, 9].

The optimization is then formulated to be

$$\begin{aligned} \vec{x}_{opt} = &\arg\min_{\vec{x}} \left[\text{LCOE}(\vec{x})\right] \\ \text{s.t.} \quad &1 \leq N_{nuclear} \leq 80 \\ &5000 \leq N_{wind} \leq 15000 \\ &100 \leq A_{solar} \leq 1000 \text{ km}^2 \\ &E_{gen}(t) - D(t) \geq 0 \quad \forall t \in [t_0, t_f], \end{aligned} \tag{7}$$

where the first three constraints are constraints on the design parameters and the final constraint ensures that the total generated energy exceeds the energy demand at all time steps. The upper and lower bounds for the design parameters were chosen as such to provide both flexibility of design in the optimization while somewhat limiting the ranges of each parameter in the interest of optimization time. The chosen values appear to provide a reasonable balance between these two considerations.

While the final constraint ensures that there will be no unmet electricity demand, there is no explicit penalty for overproducing energy. However, overproduction is effectively penalized in the calculation of the LCOE. First, the net cost of energy generation is normalized by the amount of energy demand, not the amount of energy generated. Therefore, neglecting the effect of hydrogen revenue on the calculation, producing more energy than the demand would result in growth only of the numerator while the denominator (which is in fact a constant) remains fixed. Furthermore, any excess energy production is being converted into hydrogen, either for storage or to sell. In the case of being sold, the energy produced incurs cost not only at the time of generation in either the wind, solar, or nuclear energy terms, but has the additional cost of electrolysis and storage, resulting in total costs far higher than those for energy produced and used directly to meet the electricity demand.

Finally, the actual value of the LCOE in Eq. 6 can vary significantly depending on the amount of hydrogen sold and the price it is sold at. Green hydrogen currently sells for between \$2.50/kg and \$6.80/kg [10]. If the hydrogen can be generated for sufficiently low costs and sold for sufficiently high prices, it is possible that selling the hydrogen could result in a net reduction in LCOE. This variability can be removed by assuming that the excess hydrogen is sold for exactly what is cost to produce.

In this case, it is necessary to calculate the cost to produce and store the excess hydrogen. For this, it is assumed that the energy used to make hydrogen through electrolysis comes from each energy source proportional to what is being produced by each source in that moment. That is,

$$C_{H2} = \frac{\int_{t_0}^{t_f} \left(\sum_i \dot{E}_i(t) - D(t)\right) \left(\frac{\sum_i \dot{E}_i(t)(\text{LCOE}_i + \text{LCOE}_{elec} + \text{LCOE}_{storage}}{\sum_i \dot{E}_i(t)}\right) dt}{\frac{\eta_{elec}\eta_{rect}}{e_{H2}} \int_{t_0}^{t_f} \left(\sum_i \dot{E}_i(t) - D(t)\right) dt}, \tag{8}$$

where the first term in the numerator of the integrand calculates the amount of excess power at time t, and the second term calculates the instantaneous LCOE of the system, where the summation sums over nuclear, solar, and wind energy production, and the denominator calculates the amount of hydrogen produced in kilograms. The energy density of hydrogen is taken to be $e_{H2} = 142\,\text{MJ/kg}$, η_{elec} is the electrolyzer efficiency, and η_{rect} is the efficiency of the rectifier. Thus, Eq. 8 gives the cost of produced hydrogen per kilogram.

In practice, this optimization problem is solved using a genetic algorithm, as implemented in the differential evolution function in the SciPy Python package.

5 Results and Discussion

Given the significant amount of hydrogen being sold, the effective LCOE of the system is very sensitive to the price at which the hydrogen is sold. For example, if the hydrogen were sold instead for \$2.50/kg, the bottom of the range given earlier, the LCOE would be \$92.66/MWh, a 46% increase compared to the break-even LCOE. Also, 1.83 billion kg of hydrogen amounts to 1.9% of the 98 billion kg annual global demand for hydrogen [6], which is a likely unrealistic amount of hydrogen to produce and sell.

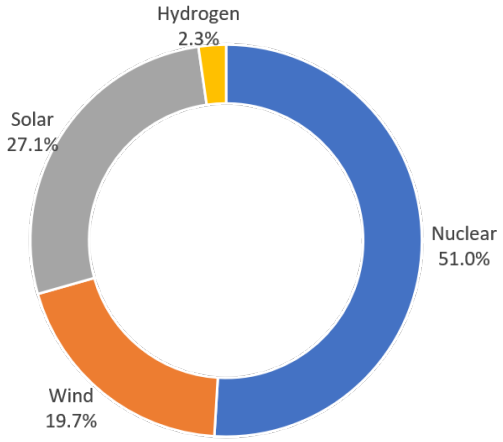

Figure 12: Proportions of energy produced by each generation method for the optimal design point.

5.1 Model Dynamics

To show how the HES subsystems work together to meet or exceed demand, two 10-day snapshots from the year are shown in Fig. 13. In the first example (Spring, Fig. 13a), demand is quite low and solar and wind output are higher than average. The result is that the nuclear power (green) is operating at steady state nearly the whole time, modulating only occasionally when demand peaks and wind valleys coincide. During this time period, the hydrogen fuel cells are not used at all. This is in stark contrast with the second example (Summer, Fig. 13b). In this example, demand is quite high, and both wind and solar output are lower than they were in the Spring example. As a result, the nuclear power is modulating significantly more to try to match the peaks and valleys in the residual demand. However, the variation in residual demand (the demand left after subtracting out the power from wind and solar) far exceeds the capabilities of the nuclear system. Each nuclear reactor is able to vary its power output between 0 and 500 MW, but the residual demand in this period ranges from -200 MW during the day to 800 MW at night. Therefore, the hydrogen storage and fuel cell systems are utilized in these periods. As solar output drops in the evening, hydrogen power increases to meet demand. During the day, the excess power is converted to hydrogen to replenish the hydrogen storage. It is also interesting to see that in Fig. 13b, the duration of boosted output from the nuclear plants is insufficient for meeting the extended periods of increased demand. This seems to suggest that it could be worthwhile to tailor the amount of thermal storage to the demand profile of its market.

The capacity factor of each subsystem differed from the assumed values in Table 1. Nuclear and wind had higher than anticipated capacity factors, with 100% and 47.4%, respectively. The capacity factors of solar, electrolysis, and fuel cells were lower than had been assumed, being 24.1%, 19.7%, and 3.1%, respectively. These capacity factors are visualized in Fig. 14. However, the capacity factor determined here for solar power is using horizontal panels rather than panels at an optimal angle. Optimally-angled panels would have a greater capacity factor. Using these true capacity factors, the LCOE can be recalculated to be \$73.04/MWh when selling the hydrogen at cost for \$6.98/kg. This is a fairly significant change in LCOE and hydrogen production cost and is something that would likely impact the results of the optimization if it were run again.

5.2 Hydrogen Storage Usage

The seasonal hydrogen storage and hydrogen fuel cells, while only contributing 2.3% of the total amount of electricity generated, were necessary for meeting the electricity demand during the summer months and during periods of particularly low solar and wind energy generation throughout the year. This is shown in Fig. 15. The storage is full for the majority of the year, with small dips on occasion. Then, over the course of about one month (mid August to mid September), the storage is used up entirely before being replenished over several weeks. During this period of heavy hydrogen use for electricity, no hydrogen is being produced to sell; all of the produced hydrogen is being used to replenish the storage tanks.

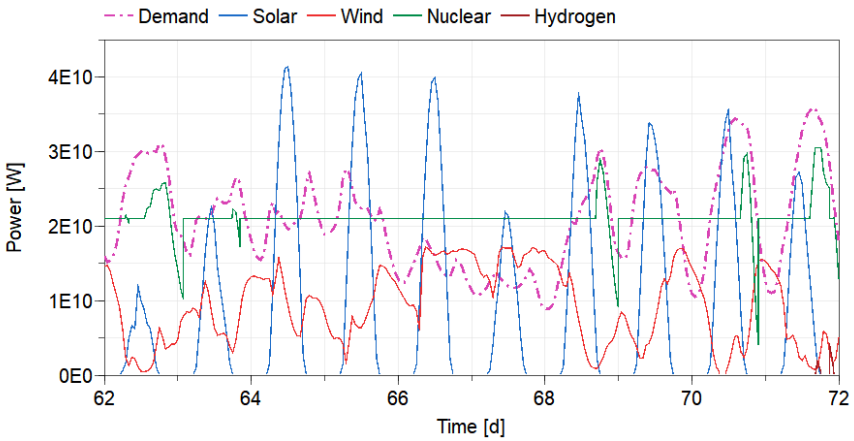

(a) Spring (Mar. 2-11)

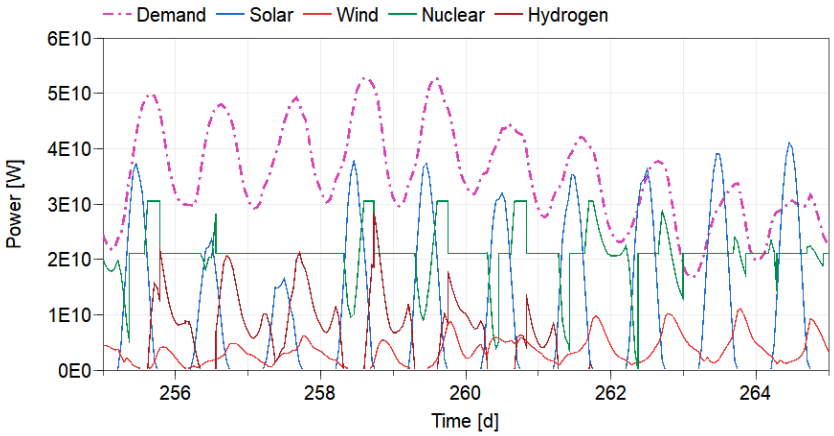

(b) Summer (Sep 11-20)

Figure 13: Ten-day snapshots of the HES dynamics, showing (a) a low-demand period in Spring and (b) a high-demand period in Summer.

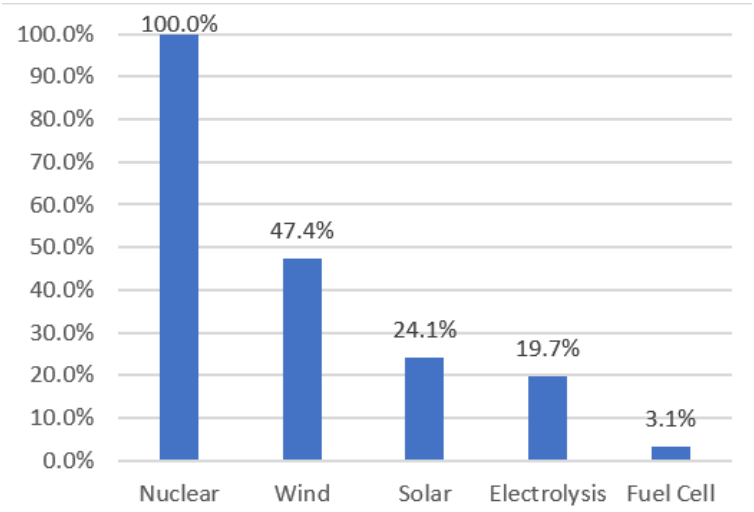

Figure 14: Capacity factor of each subsystem.

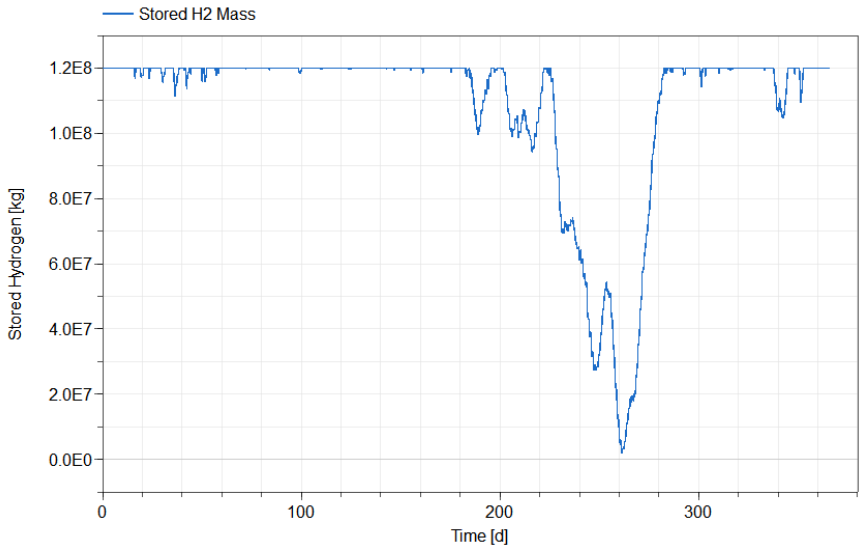

Figure 15: Level of hydrogen storage throughout the year.

The system's ability to meet these peaks in demand depend both on the maximum discharge rate of the storage and the storage capacity. Given the volatility of the residual demand, the maximum discharge rate seemed to be the more sensitive of these two parameters. It was seen that having large amounts of storage was not useful without a correspondingly large allowable discharge rate, and that having a high maximum discharge rate was generally more useful than larger storage capacity. It was through experimentation with this trade-off and a qualitative assessment of a reasonable amount of hydrogen storage capacity that the 3-day discharge rate and 20 salt caverns of storage were specified for this model.

6 Conclusions

The hybrid energy system presented in this report successfully meets the electricity demand in Texas without using fossil fuels by using a combination of wind, solar, nuclear, and hydrogen power, while also producing significant amounts of hydrogen to sell for industrial use or other purposes. However, it does not accomplish this goal particularly economically. The system has an overall LCOE of \$73.04/MWh when adjusting the subsystem LCOEs for their respective capacity factors. Given the sporadic use of hydrogen for electricity through hydrogen fuel cells, its capacity factor was extremely low, contributing significantly to the overall cost of the system while providing little return in terms of electricity production. Given the excessive cost of the hydrogen fuel cell system when using it for meeting seasonal energy demands, it would be worthwhile to explore alternative strategies for meeting this seasonal variation in demand. For example, it may in fact be cheaper to operate other primary energy generation facilities (e.g. a nuclear plant) only during seasons of higher demand than relying on seasonal energy storage. Furthermore, the assumption of being able to sell the excess hydrogen produced by the system may not be valid given the large amount of hydrogen being produced, so alternative designs or design points which produce less hydrogen overall or use a different strategy for meeting seasonal demand could eliminate this assumption.

Given the significant portion of nuclear power in the HES design, it could be beneficial to explore using these reactors in an as-needed basis instead of operating them as a must-run resource. With such significant nuclear penetration, it may no longer be feasible to run the reactors at 100% capacity all the time, discounting maintenance and refueling periods. In this way, nuclear reactors in such a system may need to operate more similarly to the current coal and natural gas energy infrastructure, in which plants will run at partial capacity during low-demand seasons and increasing to full capacity when needed.

This study could be further improved in a number of ways. First, it would be beneficial to use the adjusted subsystem LCOEs in the optimization instead of using the assumed constant values for those subsystems. The LCOE of the optimal point shown in this report was fairly different between the constant LCOE values

and the values adjusted for the true capacity factors of the subsystems. While the capacity factor of the wind, solar, and nuclear resources should not vary with the design of the system with the current model, this change would produce more accurate cost models for the hydrogen fuel cells, electrolyzer, and storage. Next, a higher-fidelity system model would allow for a more accurate depiction of how a real system would operate. For example, an explicit model the steam cycle with pump and turbine maps, modeling heat loss from the thermal storage tanks and temperature variability in the tanks, or using a solar panel model which optimally angles the panels would all be useful improvements to the current model.

Additionally, this study only considered the demand and weather data for one year. A more robust system design would need to more directly account for the volatility in wind speed, solar irradiance, temperature, demand, and the correlations between these variables. This could be accomplished by using synthetic time histories and a stochastic optimization to find robust designs with quantified uncertainty. As other time histories are considered, the aforementioned changes to account for different capacity factors becomes even more important since the capacity factors of the wind, solar, and nuclear power would also vary in this case.

Finally, one potential benefit of the HES design in this report is its ability to adapt to growing demands and growing populations. Since the system overproduces energy for much of the year, the system should be able to handle higher demand in these time periods without modification. Increasing summer demand could also be dealt with by simply expanding the hydrogen storage and fuel cell subsystems while leaving the rest of the system unchanged. In summary, the proposed HES could be a design which can flexibly grow with the population and adapt to changes in demand with minimal modifications, all while still avoiding fossil fuels.

Author Contributions and Acknowledgments

Jacob Bryan: Model development and optimization, data collection and preprocessing. Aiden Meek: Economic modeling, hydrogen system modeling, conceptual development. We would also like to acknowledge Seth Dana and Md. Sakir Islam for their assistance in developing the Dymola simulation model used in this report.

Bibliography

[1] U.S. Energy Information Administration (EIA). Texas - State Energy Profile Overview.

[2] ERCOT. Hourly Load Data Archives.

[3] NASA. NASA POWER | Prediction Of Worldwide Energy Resources.

[4] Lucas Bauer. GE General Electric GE 3.2-130 - 3,20 MW - Wind turbine, https://en.wind-turbine-models.com/turbines/1290-ge-general-electric-ge-3.2-130.

[5] Konor L. Frick, Paul W. Talbot, Daniel S. Wendt, Richard D. Boardman, Cristian Rabiti, Shannon M. Bragg-Sitton, Mark Ruth, Daniel Levie, Bethany Frew, Amgad Elgowainy, and Troy Hawkins. Evaluation of Hydrogen Production Feasibility for a Light Water Reactor in the Midwest. Technical Report INL/EXT-19-55395-Rev000, Idaho National Lab. (INL), Idaho Falls, ID (United States), September 2019.

[6] Grand View Research. Global Hydrogen Generation Market Size Report, 2021-2028, March 2021.

[7] S&P Global Platts. Atlas of Energy Transition, December 2021.

[8] R.K. Ahluwalia, D.D. Papadias, J-K Peng, and H.S. Roh. System Level Analysis of Hydrogen Storage Options. *2019 Annual Merit Review and Peer Evaluation Meeting*, page 42, April 2019.

[9] U.S. Energy Information Administration. Levelized Costs of New Generation Resources in the Annual Energy Outlook 2021. page 25, 2021.

[10] Leigh Collins. A wake-up call on green hydrogen: the amount of wind and solar needed is immense | Recharge, March 2020. Section: transition.